JOURNAL OF MATERIALS SCIENCE 12 (1977) 1392–1400

Dendrite coarsening during solidification of hypo- and hyper-eutectic Al-Cu alloys

JUNICHI KANEKO
National Research Institute for Metals, Tokyo, Japan

Dendrite coarsening during cooling at a constant rate was compared at various stages of solidification with that during isothermal holding for Al–Cu alloys of hypo- and hyper-eutectic compositions. For each specimen, the undercooling for the initial dendrite formation and the time elapsed after it were measured directly. The dendrite arm spacing was shown to be determined solely by the latter, and the dendrite structure was therefore coarsening-controlled from the early stage of solidification. The rate of coarsening in terms of the dendrite arm spacing during solidification at a constant cooling rate was same as that during isothermal holding in all the alloys tested. Numerical values of the fractional rate of solidification were evaluated for the hypo-eutectic compositions and the results show that the rate of dendrite coarsening does not depend on the fractional rate of solidification. Aluminium dendrites show structural coarsening with progressive solidification in the same way as during isothermal holding. $CuAl_2$ dendrites show curved boundaries after isothermal holding whereas those cooled at a constant rate are faceted.

1. Introduction

At the beginning of solidification, the morphology of the initially formed dendrites has been related to undercooling [1–4], or to fractional rate of solidification [5, 6]. The spacings of primary dendrite stalks in unidirectional solidification, which are considered not to vary with continuing solidification, have been related to the fractional rate of solidification, or more simply to the cooling rate [7]. As for the higher order dendrite arms, their spacing increases due to coarsening during solidification so as to reduce the total energy of solid–liquid interface [8].

The simplest case of diffusion-controlled coarsening is for particles of spherical shape where the increase of their average size can be expressed as

$$r^3 - r_0^3 = ht$$

where r and r_0 are the average radii of the spherical particles at the time for coarsening $t = t$ and 0, respectively and h is a constant [9, 10]. In case of dendrite coarsening during solidification, the geometrical situation is much more complicated, and furthermore, the fraction of solid varies appreciably with continuing solidification. In such a case, it is convenient to take the dendrite arm spacing, d, in place of the radius of dendrite arms. Thus, coarsening of dendrites will be expressed as

$$d^n - d_0^n = h't$$

where h' is a constant similar in expression to h, d and d_0 are the dendrite arm spacings at the coarsening time $t = t$ and 0 respectively, and n is also an experimentally determined constant ≈ 3, or in a range between 2.5 and 4 for various alloy systems. Here, the value of d_0 is considered to depend on the undercooling at the onset of dendrite formation. When d^n is not much greater than d_0^n, d is expressed as a function of both t and d_0 and thus d is not uniquely determined by the coarsening time. On the other hand, when d^n is much greater than d_0^n, the value of d is uniquely determined by t, and it can be said that dendrites are coarsening-controlled.

The purpose of the present work is to determine when and how the dendrites of Al–Cu alloys become coarsening-controlled by studying the coarsening behaviour at various stages of solidifi-

cation. Dendrite coarsening during cooling at a constant rate was compared with that during isothermal holding for Al–Cu alloys of hypo- and hyper-eutectic compositions.

2. Experimental procedure

Al–Cu alloys, seven of them hypo-eutectic and two of them hyper-eutectic compositions, were prepared as the test specimens. Their chemical compositions are listed in Table I, together with the liquidus temperatures, the temperature ranges of solidification and the holding temperature of the melt which were estimated from the phase diagram [11]. The alloys were made in an induction furnace using a graphite crucible, and cast into a graphite mold as bars 6 mm x 6 mm x 200 mm.

The apparatus for the solidification experiments consisted of a horizontal tubular furnace, a temperature programming unit (Chino NP163), a strip chart recorder and a water-cooled copper block for solidification interruption. A stainless steel container, in which a specimen 6 mm x 6 mm x 36 mm (4 to 6 g depending on the alloy composition) was set, was inserted at the middle of the furnace 40 cm long. The temperature of the specimen during solidification experiments was uniform within experimental accuracy. An Inconel-sheathed CA thermocouple with its junction grounded to the sheath of diameter 1.0 mm was inserted into the middle part of the specimen, and undercooling for the onset of dendrite formation and solidification time were measured for each specimen. Thermocouples used for this purpose were calibrated for the melting point of pure aluminium. Thus, the accuracy of measured temperatures was within $\pm 0.2^\circ$ C, and the true values of undercooling were considered to be obtained by the measurements under relatively slow cooling rates as in the present experiments. The stainless steel container and thermocouple were coated with a colloidal solution of boron nitride. They could be used repeatedly without any erosion by the melt of Al–Cu alloys.

Solidification experiments were done in the following ways. The specimen was melted at a heating rate of 300° C h^{-1} and held at the temperatures listed in Table I for 1 h before starting cooling. Some of the specimens were cooled at constant rates ranging from 6 to 300° C h^{-1}. When cooled down to the predetermined temperature, solidification was interrupted by pulling the specimen container out of the furnace onto a water-cooled copper block. After this operation about 10 sec elapsed before complete solidification of the specimen. The other specimens were cooled at 200° C h^{-1} to the predetermined temperature, and held at this temperature for various periods. Finally, the specimen was quenched the same way as above. In this way, dendrite coarsening during cooling at a constant rate was compared with that during isothermal holding at various stages of solidification.

After solidification experiments, these specimens were cut at the cross sections 2 to 3 mm from the position where a thermocouple was inserted, and the dendrite structure was examined under an optical microscope. Measurements of dendrite arm spacings were made by a micrometer attached to the microscope for more than 20 dendrites of each specimen whose primary arms were nearly parallel to the plane of metallographic obsefvation, and the average value was taken.

3. Experimental results

3.1. Hypo-eutectic alloys

The values of the dendrite arm spacing for alloys of seven different compositions, cooled at constant rates till completely solidified, are shown in

TABLE I Alloy composition, liquidus temperature, range of solidification temperatures and temperature for holding the melt for each specimen.

Alloy	%Cu	%Fe	T_L(°C)	$T_L - T_E$	melting (° C)
2.5% Cu	2.47	0.014	653	105	700
4.5% Cu	4.45	0.018	647	99	700
10% Cu	10.00	0.016	632	84	700
15% Cu	14.80	0.008	618	70	700
20% Cu	19.67	0.015	602	54	620, 700
25% Cu	24.70	0.018	585	37	600, 700
30% Cu	30.84	0.024	563	15	600, 700
36% Cu	35.95	0.017	558	10	600
40% Cu	39.69	0.027	569	21	600

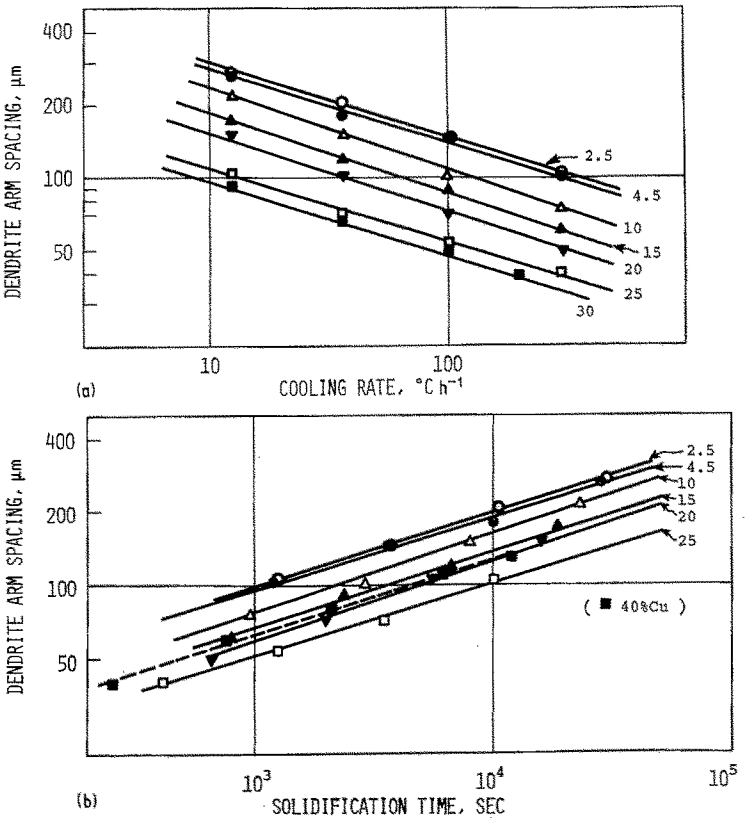

Figure 1 Dendrite arm spacings of hypo-eutectic Al–Cu alloys solidified at various cooling rates plotted against (a) cooling rate and (b) solidification time.

Fig. 1. As shown in Fig. 1(a), the dendrite arm spacing decreases with increasing Cu content for a given cooling rate, and is given by parallel straight lines in logarithmic plotting, in agreement with previous work [12]. By taking solidification time, as in Fig. 1(b), these parallel lines come closer each other, but for a given solidification time, the dendrite arm spacing is still smaller for the higher Cu content. The average slope of the lines shown in Fig. 1(b) is about 0.3, and these also agree with the previous reports [13, 14].

Changes of the dendrite morphology during solidification of an Al–15% Cu alloy under a constant cooling rate of 36° C h^{-1} are shown in

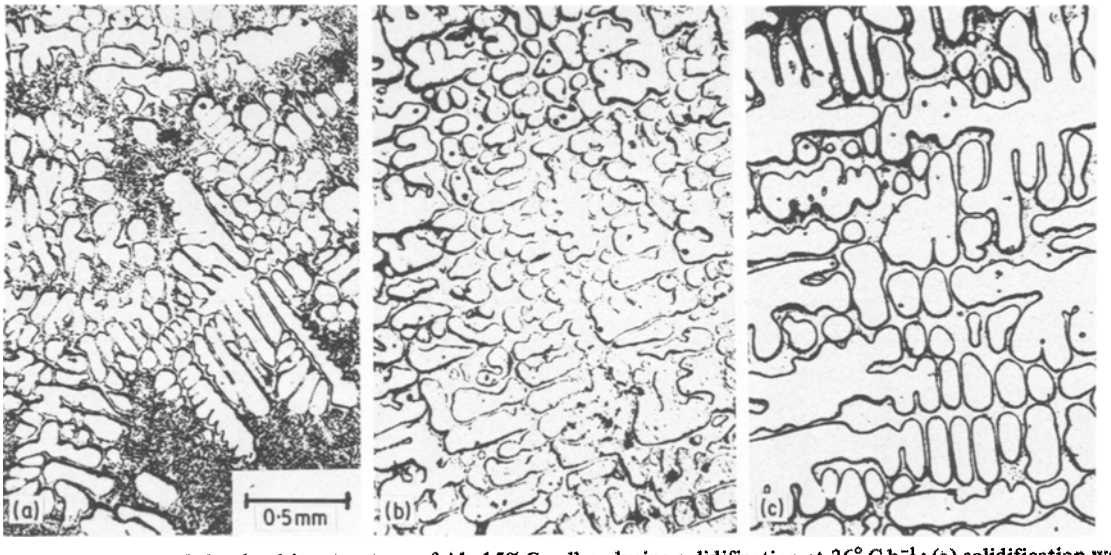

Figure 2 Changes of the dendrite structure of Al–15% Cu alloy during solidification at 36° C h^{-1}; (a) solidification was interrupted at 607° C, (b) at 590° C, (c) after complete solidification.

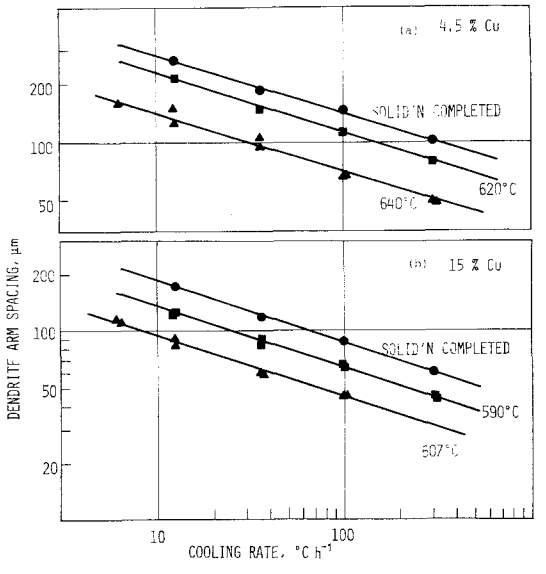

Figure 3 Dendrite arm spacings at various stages of solidification at constant cooling rate, (a) Al–4.5% Cu, (b) Al–15% Cu.

Fig. 2. The increase in the volume fraction of aluminium dendrites, as well as their structural coarsening, is clearly seen with progressive cooling. Dendrite arm spacings of the specimens obtained by solidification interruption after cooling at constant rates are shown in Fig. 3 for Al–4.5 and 15% Cu alloys. For both alloys, a straight line was obtained on a log/log plot for each temperature of solidification interruption, and these lines are parallel to each other. For alloys containing more than 20% Cu and temperatures near the liquidus line the lines are not parallel to those for lower temperatures. As will be shown below, this is simply because undercooling for the onset of dendrite formation, which is larger for higher Cu content, increases with increasing cooling rate.

Changes of the dendrite structure during isothermal holding at a temperature in the solidification range are shown in Fig. 4 for Al–10% Cu specimens held at 622° C (10° C below the liqui-

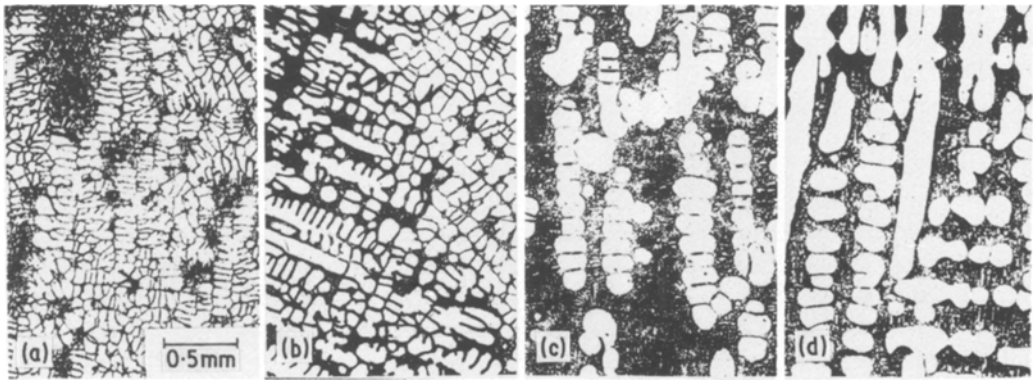

Figure 4 Changes of the dendrite structure of Al–10% Cu during isothermal holding at 622° C after cooling at 100° C h^{-1}. Specimens were quenched after holding for (a) 0 min, (b) 7.5 min, (c) 29.4 min, (d) 63 min.

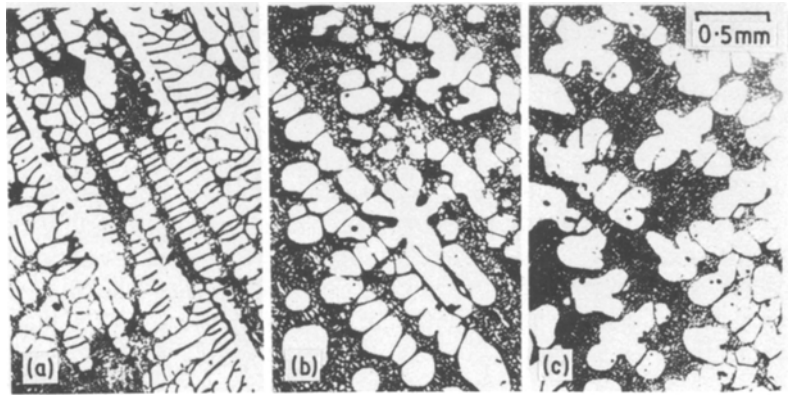

Figure 5 Dendrite structure of Al–10% Cu cooled at various rates to 622° C and quenched, (a) 36° C h^{-1} and equal solidification time as in Fig. 4(b), (b) 12.5° C h^{-1} and equal solidification time as in Fig. 4(c), (c) 6.25° C h^{-1} and equal solidification time as in Fig. 4(d).

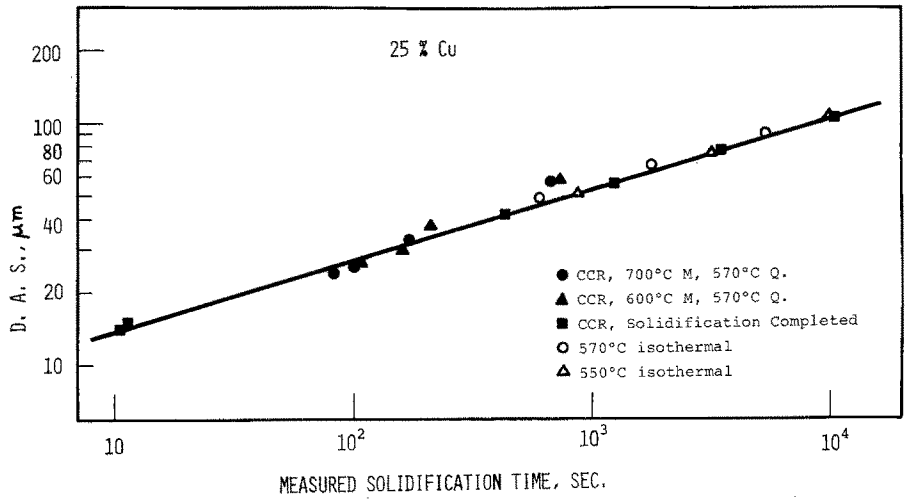

Figure 6 Dendrite arm spacings of Al–25% Cu solidified under various conditions.

dus temperature, T_L) after cooling at 200° C h^{-1}. Fig. 5 shows the dendrite structure of the specimens cooled at various rates down to 622° C so as to give equal solidification times with those in Fig. 4. By comparing Figs. 4 and 5, no significant difference in the dendrite structure is observed between the specimen cooled at a constant rate and that isothermally held, for the same solidification time.

Dendrite arm spacings of Al–25% Cu specimens made under various conditions are plotted against the measured solidification times in Fig. 6. For all Al–25% Cu specimens obtained in the present experiments, the value of the dendrite arm spacing is uniquely determined by the solidification time, and hence the dendrites are already coarsening-controlled when cooled to 570° C (15° C below T_L) at constant rates. Similar plots have been obtained for all the other hypo-eutectic alloys. The dendrite structure is observed to be coarsening-controlled when the specimens are cooled at constant rates down to 646° C for Al–2.5% Cu, to 640° C for Al–4.5% Cu, to 622° C for Al–10% Cu, to 607° C for Al–15% Cu, to 590° C for Al–20% Cu, to 570° C for Al–25% Cu and to 550° C for Al–30% Cu. Taking undercooling for the onset of solidification into account, it is concluded that dendrites of primary aluminium become coarsening-controlled at the early stage of solidification.

3.2. Hyper-eutectic alloys

Coarsening was also observed for the primary dendrites of $CuAl_2$ phase with continuing solidification. In Fig. 7, dendrites of Al–36% Cu alloy for which solidification was interrupted after cooling down to 553° C, are compared with those isothermally held at 553° C for the equal solidification time. As shown in these micrographs, the morphology of $CuAl_2$ dendrites is different from that of aluminium. The boundaries of $CuAl_2$ dendrites tend to be straight whereas those of aluminium dendrites are curved. $CuAl_2$ dendrites are considered to show the boundaries of somewhat faceted nature. However, as shown in Fig. 7, these dendrite boundaries become more curved when they are coarsened isothermally. For $CuAl_2$ dendrites, it is suggested that coarsening leads to curved boundaries, whereas growth leads to faceted ones.

Dendrite arm spacing of Al–40% Cu made under various conditions is shown against measured solidification time in Fig. 8. The dendrite arm spacings for Al–36% Cu almost coincided with the line of this figure showing that dendrite arm spacing of hyper-eutectic Al–Cu alloy is also determined solely by the solidification time. Although there exists a morphological difference between $CuAl_2$ dendrites cooled at a constant rate and those held isothermally, their structure is principally coarsening-controlled from the relatively early stage of solidification; that is, when cooled at constant rates to 553° C for Al–36% Cu and to 560° C for Al–40% Cu. Dendrite arm spacing of Al–40% Cu are plotted in Fig. 1(b) for comparison with those of hypo-eutectic alloys: the slopes for Al–40% Cu and hypo-eutectic alloys are the same.

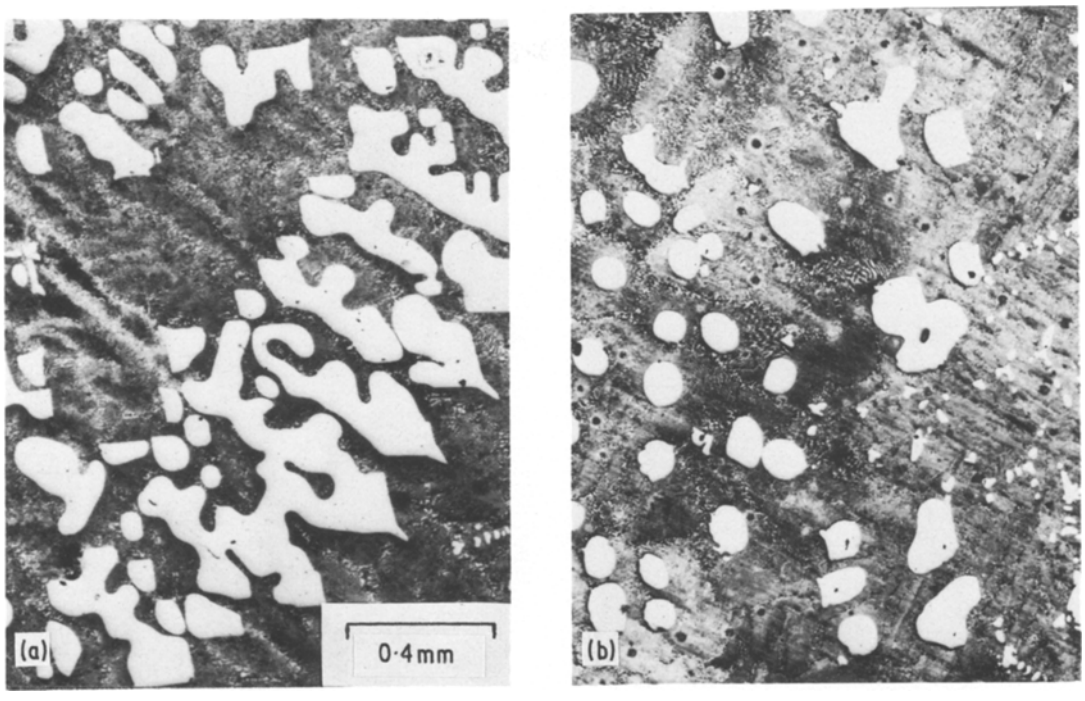

Figure 7 Dendrite structure of Al–36% Cu; (a) cooled at 6.25° C h^{-1} down to 553° C, (b) held at 553° C for 27 min after cooling at 100° C h^{-1}.

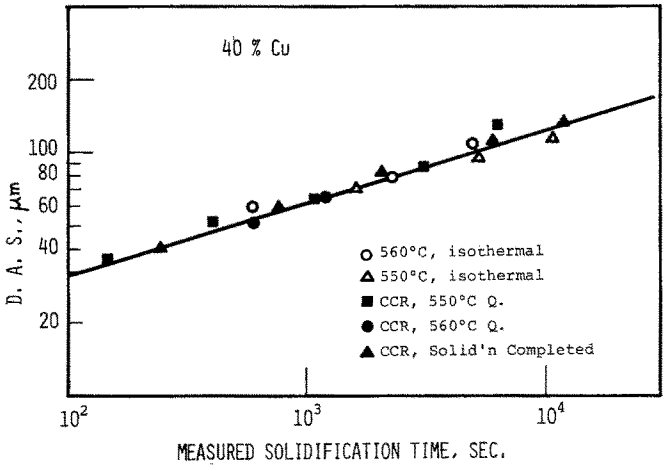

Figure 8 Dendrite arm spacing of Al–40% Cu solidified under various conditions.

3.3. Undercooling

Two kinds of undercooling were measured; one for the onset of dendrite formation, ΔT_L, and the other for the start of solidification of the remaining eutectic melt, ΔT_E. The values of ΔT_L and ΔT_E obtained for hypo-eutectic alloys are shown in Fig. 9 for a cooling rate of 200° C h^{-1}. With increasing Cu content ΔT_L increases, whereas ΔT_E decreases. As shown in Fig. 10, ΔT_L depends not only on the cooling rate but also on the superheating of the melt before solidification for Al–25% Cu. ΔT_L increases with increasing cooling rate, and is larger for a higher amount of superheating. In fact, ΔT_L possibly depends on the other factors which would influence the nucleation behaviour of the primary solid phase in the melt, such as the amount of some impurity elements or the surface conditions of the melt container. The structure of the dendrites initially formed is considered to depend on ΔT_L. However, it is obvious from the results shown in Fig. 6 that dendrite arm spacings, when measured some time after the onset of dendrite formation, do not depend on ΔT_L and are determined solely by the time elapsed after the onset of dendrite formation.

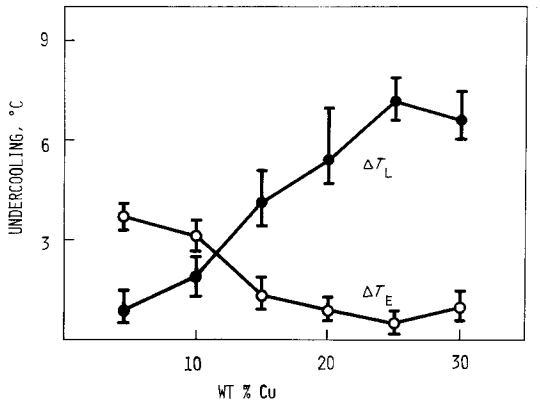

Figure 9 Measured values of undercooling for the onset of dendrite formation, ΔT_L, and those for eutectic solidification, ΔT_E, plotted against Cu content. Specimens were cooled at 200° C h^{-1} from 700° C.

4. Discussion

4.1. Effect of the fractional rate of solidification

Proposed models of dendrite coarsening [8, 15] have been discussed quantitatively only in terms of isothermal coarsening; the effect of solidification rate is not taken into account. However, the increase of the fractional rate of solidification should decrease the rate at which smaller dendrite arms disappear, and thus to retard dendrite coarsening.

Dendritic solidification of a simple binary system such as Al–Cu proceeds approximately according to the well-known Scheil equation [16, 17]

$$C_s = kC_0(1-f_s)^{k-1}$$

where C_s is the solute concentration of solidifying solid, C_0 the overall composition, k the equilibrium coefficient and f_s the fraction of solid. Upon cooling at a constant rate, the fractional rate of solidification, df_s/dt is proportional to df_s/dT, where t and T are time and temperature, respectively. From the above equation, df_s/dT is obtained as

$$\frac{df_s}{dT} = \frac{1}{k-1}\frac{1}{T_0-T_L}\left[\frac{T_0-T_L}{T_0-T}\right]^{\frac{k-2}{k-1}}$$

where T_0 is the melting point of the pure solvent.

Numerical values of df_s/dT were calculated for the various hypo-eutectic Al–Cu alloys and the results obtained are shown in Fig. 11. Here, the remaining part of the melt of the eutectic composition and undercooling for the onset of solidification were not taken into consideration. For each alloy, df_s/dT is maximum at T_L and decreases with continuing solidification. With decreasing Cu content, df_s/dT at T_L increases, but the decreasing rate of df_s/dT upon cooling is appreciably higher for lower Cu content. In high Cu alloys, df_s/dT is initially low and it decreases only gradually with continuing solidification at

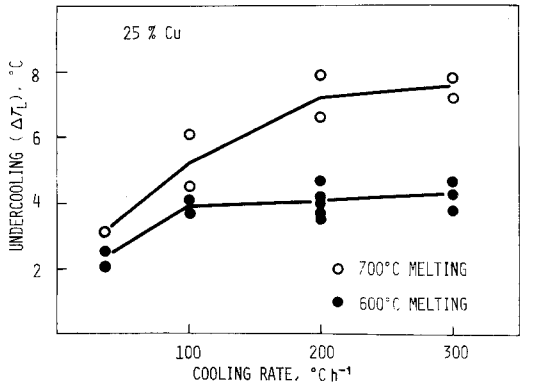

Figure 10 Measured values of ΔT_L in Al–25% Cu plotted against cooling rate for different superheating of the melt.

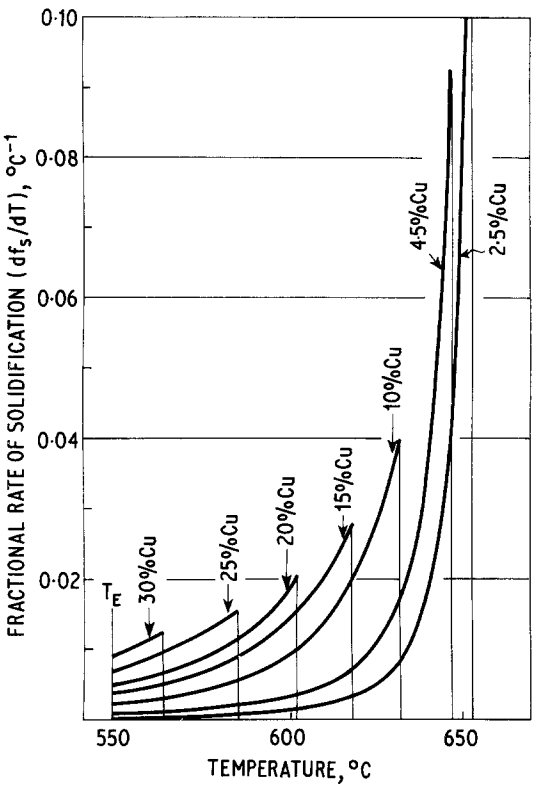

Figure 11 Fractional rate of solidification during cooling at a constant rate plotted against temperature for various hypo-eutectic Al–Cu alloys.

a constant cooling rate. However, for all the hypo-eutectic alloys tested, dendrite coarsening was shown to occur at the same rate as that during isothermal holding where the fraction of solid was kept unchanged. Thus, the rate of dendrite coarsening did not depend on the fractional rate of solidification in the range of the present experiments.

4.2. Coalescence of dendrite arms

The preceding discussion suggests that the smaller dendrite arm spacing for the higher Cu content at a given solidification time cannot be attributed to the fractional rate of solidification. An alternate explanation for this is possible by considering coalescence of neighboring dendrite arms since it occurs preferentially in low Cu alloys where the boundaries of neighboring arms stay closer [13]. Such coalescence has been claimed to play an important role in dendrite coarsening [18].

The above experimental results show that the difference in the rate of dendrite coarsening between high and low Cu alloys is small, although coalescence of dendrite arms is unlikely to occur in high Cu alloys. The dendrite structure of Al–4.5% Cu cooled at $100^\circ C\,h^{-1}$ to complete solidification is shown in Fig. 12. Such micrographic observation reveals that coalescence occurs only when the temperature approaches the eutectic point in low Cu alloys. The dendrite structure of the same alloy held at 640° C shows that coarsening takes place without any appreciable accompanying coalescence. The coarsening rate in terms of the dendrite arm spacing is the same for a specimen cooled at a constant rate as for one held isothermally. This is attributed to the fact that liquid particles, trapped in the solid by coalescence of neighbouring arms and concentration gradients of the solute around them, are usually taken into account in measuring the dendrite arm spacing. However, the marked difference in the dendrite structure between high and low Cu alloys after complete solidification is attributed to coalescence occurring in the latter. Coalescence is therefore considered to play an important role in determining the dendrite structure of low Cu alloys as previously pointed out [19]. On the other hand, coalescence plays a rather minor part in dendrite coarsening when it is considered in terms of the dendrite arm spacing as in the present study.

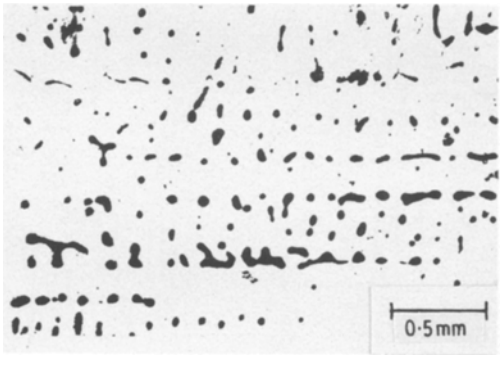

Figure 12 Coalesced dendrite structure of Al–4.5% Cu after complete solidification at $100^\circ C\,h^{-1}$.

5. Conclusions

(1) The dendrite arm spacing of hypo- and hyper-eutectic Al–Cu alloys is shown to be coarsening-controlled from the early stage of solidification.

(2) Aluminum dendrites show structural coarsening with continuing solidification at a constant cooling rate in the same way as those during isothermal holding. In contrast to this, $CuAl_2$ dendrites after isothermal holding show curved boundaries whereas those cooled at a constant rate are faceted.

(3) The amount of ΔT_L increases with increasing either Cu content in the hypo-eutectic range or the cooling rate. ΔT_L also depends on the amount of superheating of the melt before solidification. Irrespective of ΔT_L, the dendrite arm spacing is determined solely by the time elapsed after the onset of dendrite formation.

(4) The relative values of the fractional rate of solidification have been obtained for the hypo-eutectic Al–Cu alloys. The rate of coarsening in terms of the dendrite arm spacing during solidification at a constant cooling rate is same as that during isothermal holding in all the alloys tested. Thus, the rate of dendrite coarsening does not depend on the fractional rate of solidification.

(5) Coalescence of dendrite arms occurs in low Cu alloys when the temperature approaches near the eutectic point. Such coalescence is considered to play a minor role in dendrite coarsening in terms of the dendrite arm spacing. However, the marked difference in the dendrite structure of high and low Cu alloys after complete solidification is attributed to coalescence occurring in the latter.

Acknowledgements

The author is grateful to Mr M. Takahashi for his experimental assistance and to Mr M. Hayashi for the line drawing of the figures.

References

1. W. W. MULLINS and R. F. SEKERKA, *J. Appl. Phys.* **34** (1963) 323, **35** (1964) 444.
2. R. F. SEKERKA, *ibid.* **36** (1965) 264.
3. *Idem, J. Phys. Chem. Solids* **28** (1967) 983.
4. *Idem, J. Crystal Growth* **3** (1968) 71.
5. P. E. BROWN and C. M. ADAMS, *Trans. Am. Foundrymen's Soc.* **69** (1961) 879.
6. P. K. ROHATGI and C. M. ADAMS, *Trans. Met. Soc. AIME* **239** (1967) 1737.
7. M. C. FLEMINGS, "Solidification Processing" (McGraw-Hill, New York, 1974)
8. T. Z. KATTAMIS, J. C. COUGHLIN and M. C. FLEMINGS, *Trans. Met. Soc. AIME* **239** (1967) 1504.
9. A. J. ARDELL and R. B. NICHOLSON, *J. Phys. Chem. Solids* **27** (1966) 1793.
10. A. J. ARDELL, "Mechanisms of Phase Transformation in Crystalline Solids" (Inst. Metals, London, 1969) p. 111.
11. "Equilibrium Diagrams of Aluminium Alloy Systems", Bulletin 25, (Aluminium Dev. Assoc. London, 1961).
12. J. A. HORWATH and L. F. MONDOLFO, *Acta Met.* **10** (1962) 1037.
13. K. H. CHIEN and T. Z. KATTAMIS, *Z. Metallk.* **61** (1970) 475.
14. N. MORI, K. OGI and K. MATSUDA, *J. Japan Inst. Metals* **40** (1976) 406.
15. M. KAHLWEIT, *Scripta Met.* **2** (1968) 251.
16. H. D. BRODY and M. C. FLEMINGS, *Trans. Met. Soc. AIME* **236** (1966) 615.
17. T. F. BOWER, H. D. BRODY and M. C. FLEMINGS, *ibid.* **236** (1966) 624.
18. K. P. YOUNG and D. H. KIRKWOOD, *Met. Trans.* **6A** (1975) 197.
19. S. V. SABRAMANIAN, C. W. HAWORTH and D. H. KIRKWOOD, *J. Iron Steel Inst.* **206** (1968) 1027.

Received 17 September and accepted 2 December 1976.